

# Sand Transport in Nile River, Egypt

S. Abdel-Fattah<sup>1</sup>; A. Amin<sup>2</sup>; and L. C. Van Rijn<sup>3</sup>

**Abstract:** Measurements of bed-load and suspended-load transport rates were carried out successfully at four cross sections of the Nile River, in Egypt, along the entire length from Aswan to Cairo using a mechanical sampler called the Delft Nile Sampler. The measured transport rates were compared to similar data sets from two other large scale rivers: the Rhine-Waal River in the Netherlands and the Mississippi River in the USA. The bed-load transport rates in the Nile River and in the Rhine-Waal River are in very good agreement. Comparison of suspended transport rates in the Nile River and in the Mississippi River shows that both data sets are complementary, revealing a very consistent trend of suspended transport against current velocity; suspended transport is roughly proportional to  $(V_{av})^{3 \text{ to } 4}$ . Three formulas for the prediction of bed-load transport were tested using the Nile data: Meyer-Peter–Muller, Bagnold, and Van Rijn. The prediction formula of Van Rijn produced significantly better results than the other two formulas; the average relative error was about 60%. The formula of Van Rijn was modified to extend it to conditions with slightly nonuniform sediment mixtures by introducing a correction factor for the bed shear parameter. Based on a limited number of flume experiments, the correction factor was found to be dependent on the characteristics of the sediment mixture ( $d_{10}$ ,  $d_{50}$ ,  $d_{90}$ , and  $\sigma_g$ ). Comparison of bed-load transport measured in the Nile River with computed transport rates of the modified formula showed improved results; the average relative error decreased to about 30%. The formulas of Bagnold and Van Rijn were also used to compute the suspended transport rates in the Nile River. The computed transport rates were found to be within a factor of 2 of measured values; the formula of Bagnold performed slightly better. The total load transport formula of Engelund–Hansen was also successfully used (computed values within a factor of about 2 of measured values).

**DOI:** 10.1061/(ASCE)0733-9429(2004)130:6(488)

**CE Database subject headings:** Sand; Egypt; Bed load; Transport rate; Nile River; Measurement.

## Introduction

The last secret of the Nile is the amount of sand carried by the river from High Aswan Dam to the sea. This value is estimated to be in the range of 10–100 kg/s, but the exact quantity is unknown. Furthermore, it is unknown which part of the total sand load is transported as bed load and which part as suspended load.

In 1968 the High Aswan Dam (HAD) was built to regulate the water supply in the river. The dam has enabled Egypt to obtain a steady annual supply of 55.5 billion m<sup>3</sup> of water. This is particularly important since the Egyptian population is increasing steadily, which means that the country requires more and more food and energy.

The flow regime imposed by HAD has resulted in significant changes in those variables that reflect the geomorphic and hydraulic response of the river. The dam has affected the regime of the Nile and resulted in lowering of both water and bed levels downstream of the barrages. Before the construction of HAD the Nile River experienced a large range of discharges (80–900 million m<sup>3</sup> per day) and a corresponding large range in velocities. At low

flows the predominant bed form type is dunes of various sizes with megaripples superposed and large sand bars. The dunes are much longer than the water depth; the megaripples have a length of about the water depth. At high discharges the energy of flow tends to wash out the dunes of the main channel and the predominant bed form type becomes transitional dunes with megaripples. Megaripples have a length scale of about the water depth, whereas dunes have a length scale much larger than the water depth and ripples much smaller than the water depth. After the construction of HAD, the predominant bed form type is dunes due to the controlled maximum flows. Maximum velocities are reduced and have a magnitude on the order of 1.0–1.5 m/s instead of 1.5–2.0 m/s before HAD construction (Gaweesh and Gasser 1991).

The suspended-load measurements before HAD construction, at Gaafra (km 34, below Aswan), revealed that sediment concentrations were as large as about 4 kg/m<sup>3</sup> during the periods of high flow. After the construction of HAD, maximum concentrations are only in the range 0.03–0.1 kg/m<sup>3</sup>.

The basic objective of the study is to determine the total sediment load in the Nile River as a function of flow parameters; to determine the relative contributions of bed-load and suspended-load transport, and to determine the predictive skills of various sediment transport formulas for the Nile River. As the wash load is negligibly small, the present data only refer to the bed material load.

Measured bed-load and suspended-load transport rates are discussed in this paper and compared to computed transport rates. Measured transport rates of two other large rivers are shown for comparison with the Nile data. The applied sand transport models were selected because they are well-known and they represent the two main types of models: based on bed-shear stress (Meyer-

<sup>1</sup>Associate Professor, Hydraulics Research Institute, Delta Barrage 13621, Egypt.

<sup>2</sup>Research Assistant, Hydraulics Research Institute, Delta Barrage 13621, Egypt.

<sup>3</sup>Senior Hydraulics Engineer, Delft Hydraulics, P.O. Box 177, 2600 MH, Delft, The Netherlands.

Note. Discussion open until November 1, 2004. Separate discussions must be submitted for individual papers. To extend the closing date by one month, a written request must be filed with the ASCE Managing Editor. The manuscript for this paper was submitted for review and possible publication on June 6, 2001; approved on October 10, 2003. This paper is part of the *Journal of Hydraulic Engineering*, Vol. 130, No. 6, June 1, 2004. ©ASCE, ISSN 0733-9429/2004/6-488–500/\$18.00.

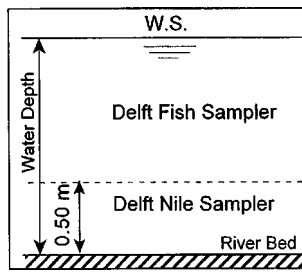


Fig. 1. Sketch of measuring technique

Peter-Muller and Van Rijn) and energy (Bagnold and Engelund-Hansen). The effect of the nonuniformity of the bed material on the transport rate is studied using data from both laboratory and field conditions. Finally, some details of the suspended sediment concentration distributions in the Nile River are discussed. Future research will focus on the details of the processes of sand transport and sorting over dunes.

## Field Measurements

### Measurement Techniques

The sediment-load transport was measured using the Delft-Nile Sampler (Van Rijn and Gaweesh 1992; Van Rijn 1993a), which was operated from an anchored boat. This mechanical sampler was designed to measure, in contact to the bed, the bed load and the suspended load up to 0.5 m above the bed (the sampler height). Three small propeller meters were attached to the sampler to measure the current velocities at 0.18, 0.37, and 0.50 m above the bed. The bed-load transport is defined as the transport between the bed surface and the top of the intake opening of the bed-load sampler (about 0.055 m). This application of this practical definition may result in some oversampling, as part of the suspended sediment is trapped. However, a special patch of 0.5 mm mesh size was used at the upper side of the bed load bag to allow the suspended sediment to leave the bag. The oversampling error is estimated to be of the order of 10–20% [see Gaweesh and Van Rijn (1994); and Kleinhans and Ten Brinke (2001)]. The suspended sand transport is defined as the transport between the top of the intake opening of the bed-load sampler and the water surface.

A separate device (Delft fish) equipped with a small nozzle connected to a suction pump, a propeller meter, and an echo sounder for depth determination was used to measure suspended load at different water depths above the bed and near the water surface, Fig. 1.

The locations of the measurement cross sections were selected in a stable reach to avoid nonsteady bed conditions during the measurements. The sites are Aswan km 15, Quena km 288, Sohag km 444, and Bani-Sweif km 828 measured downstream of the High Aswan Dam see also Fig. 3. For each measurement site, echo sounding for the cross-section profile was performed. The cross-section profile was subdivided into six measurement stations, based on statistical error analysis (Gaweesh and Van Rijn 1994). A longitudinal echo sounding profile over at least 100 m length was conducted at the location of each station to an estimate of the local bed form dimensions. The positioning of the boat was determined using a laser range finder with respect to fixed stations

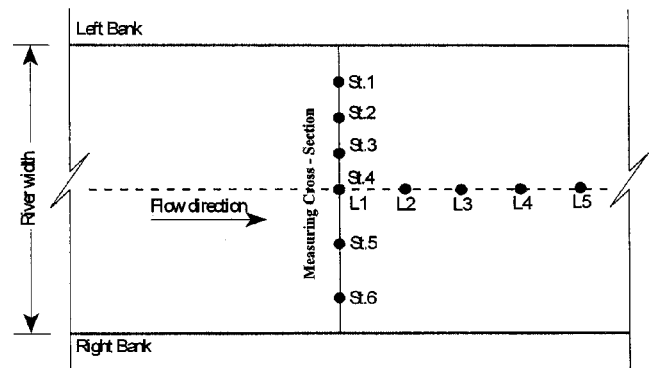


Fig. 2. Layout of measurement stations and locations

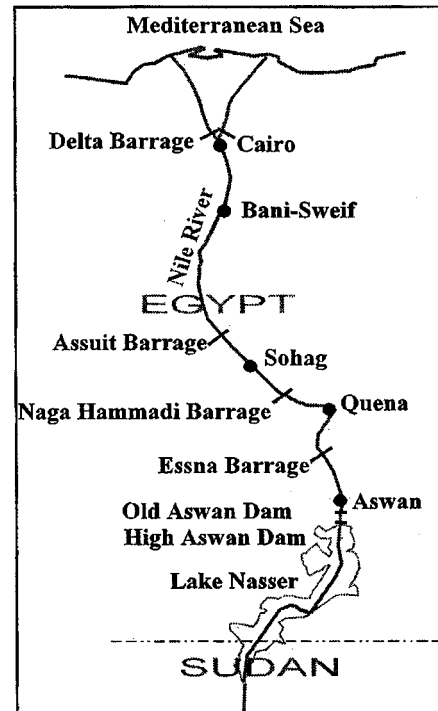


Fig. 3. Measurement locations along Nile River

Table 1. Main Characteristics of the Measurement Sites

Site	Aswan	Quena	Sohag	Bani-Sweif
River width (m)	517	578	481	400
Local slope (cm/km)	3.5	4.2	5.7	8.5
Flow discharge (m <sup>3</sup> /s)	1,331	1,250	1,560	1,040
Average bed form length (m)	44	22	24	28
Average bed form height (m)	1.6	0.8	0.7	0.75

on the bank of the river (accuracy of about 0.1 m in cross-river direction and 1 m in longitudinal direction; bed form length of about 50 m).

The local water surface slope was determined by measuring the water level at two points with a distance of about 1000 m. The flow discharge was derived from the velocity measurements at various stations across the river. During the measurement period the local water surface slope, water level, and flow discharge at the measurement site were almost constant.

**Table 2.** Measured Data per Station at Aswan

Station	Distance from (L.B.)	Mean depth (m)	$d_{10}$ ( $\mu\text{m}$ )	$d_{50}$ ( $\mu\text{m}$ )	$d_{90}$ ( $\mu\text{m}$ )	Standard deviation of bed material $\sigma_g$	Mean $K_s$ (m)	Velocity (m/s)		Suspended load (kg/m/s)		Bed load (kg/m/s)	
								Mean	Standard deviation	Mean	Standard deviation	Mean	Standard deviation
1	60	4.98	207	313	493	2.0	0.097	0.482	0.0310	0.0078	0.0008	0.0056	0.0053
2	140	5.72	187	322	580	1.8	0.086	0.487	0.0336	0.0081	0.0004	0.0012	0.0008
3	220	4.78	215	359	577	1.7	0.026	0.587	0.0085	0.0089	0.0009	0.0038	0.0033
4	300	5.02	234	389	635	2.0	0.100	0.618	0.0312	0.0098	0.0006	0.0058	0.0028
5	380	4.82	266	542	1197	1.9	0.147	0.591	0.0198	0.0092	0.0010	0.0113	0.0080
6	460	5.70	186	345	735	2.5	0.188	0.415	0.0298	0.0077	0.0006	0.0005	0.0005

The measurements of bed, suspended load, and velocity profiles were conducted at the six measurement stations (St1 to St6, see Fig. 2). At each station (St1 to St6), measurements were performed at five locations (L1, L2, L3, L4, and L5) distributed over the length of the longitudinal section which is about equal to the mean bed form length. Fig. 2 shows the layout of the measurement stations and locations. In all, measurements were performed at 30 locations. At each station the following measurements were performed for the five locations:

1. Ten instantaneous samplings using the Delft Nile Sampler with a bag of mesh size 250  $\mu\text{m}$ ; the sampler was lowered to the bed and immediately raised up after the nozzle had touched the bed ("zero"-samplings; these values are subtracted from the bed-load samplings of 3 min to correct for the initial disturbance effect).
2. Eight bed-load samplings of 3 min each using the Delft Nile Sampler with the same bag size.
3. Suspended-load samplings over the water depth using the Delft Nile and the Delft Fish Samplers. The suction of the samples was driven by a set of pulsation pumps. The samples were collected (volume=5 L) in plastic buckets.
4. Velocity profiles over the water depth using propeller current meters installed on the Delft Nile and the Delft Fish Samplers. The flow velocity measurements were carried out as follows:
  - At 0.18, 0.37, and 0.50 m above the bed level by using three propeller-type current meters attached to the Delft Nile Sampler; and
  - From 0.50 m above the bed level to the water surface by using a propeller-type current meter attached to the Delft Fish.
5. One bed material sample at the end of each measurement using a grab sampler.
6. Water temperature was measured.
7. At each station, a longitudinal bed profile for the five locations was sounded.

All bed-load samples, taken at each location in the measurement station, are separately dried and weighed and then put together to obtain a bulk sample which represents the bed-load material at the measurement station. The bed material samples for the five locations, at each measuring station, were also put together to obtain a bulk sample which represents the bed material at each station. The samples of each station were analyzed. The suspended sediment particles obtained by the Delft Nile Sampler and Delft Fish were analyzed separately (bulk samples) to determine the fall velocity by settling tube analysis.

### Description of Measurement Sites

The sediment discharge measurements were carried out at four cross sections on the Nile River covering the entire length from Aswan to Cairo. The measurements were carried out at Aswan km 15, Quena km 288, Sohag km 444, and Bani-Sweif km 828 measured downstream of the High Aswan Dam (HAD), see Fig. 3. The main topographic and hydraulic characteristics of the four measurement sites are summarized in Table 1.

The measured data are presented in Tables 2–5. The effective bed roughness height according to Nikuradse ( $k_s$ ) was obtained from data fitting of velocity measurements for all the locations of each station (Van Rijn 1990, 1993b). The values of water depths, the bed material characteristics  $d_{10}$ ,  $d_{50}$ ,  $d_{90}$  ( $d_{10}$  means that 10% of the sample is smaller than this diameter, etc.), and the bed roughness  $k_s$  for all the locations were averaged and are shown in the tables for each measurement station. The mean and standard deviation values of the flow velocity, suspended load, and bed load for each station are shown in the tables as well. The bed-load and suspended-load transport are defined in the section on measurement techniques. The tables also indicated that the standard deviation values ( $\sigma_g = \frac{1}{2}d_{84}/d_{50} + \frac{1}{2}d_{50}/d_{16}$ ) of the bed material are in the range from 1.1 to 2.5. Therefore the bed material is considered slightly nonuniform ( $\sigma_g < 3$ ). For more details see Abdel-Fattah (1997a,b,c,d); and Gaweesh et al. (1994).

**Table 3.** Measured Data per Station at Quena

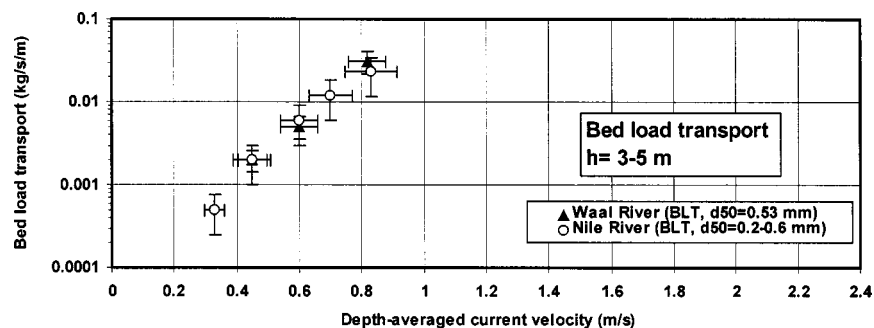
Station	Distance from (L.B.)	Mean depth (m)	$d_{10}$ ( $\mu\text{m}$ )	$d_{50}$ ( $\mu\text{m}$ )	$d_{90}$ ( $\mu\text{m}$ )	Standard deviation of bed material $\sigma_g$	Mean $k_s$ (m)	Velocity (m/s)		Suspended load (kg/m/s)		Bed load (kg/m/s)	
								Mean	Standard deviation	Mean	Standard deviation	Mean	Standard deviation
1	81	4.34	231	378	556	1.2	0.20	0.66	0.033	0.034	0.0073	0.0167	0.0134
2	164	4.65	141	282	429	2.0	0.07	0.67	0.0313	0.033	0.0058	0.0120	0.0026
3	252	4.40	166	267	389	1.5	0.10	0.60	0.0124	0.010	0.0031	0.0064	0.0052
4	338	3.55	161	277	354	1.5	0.11	0.49	0.0236	0.006	0.0011	0.0015	0.0006
5	414	4.03	135	239	315	1.6	0.23	0.31	0.0121	0.003	0.0003	0.0001	0.0001
6	517	3.88	184	267	344	1.4	0.35	0.36	0.0159	0.003	0.0003	0.0009	0.0013

**Table 4.** Measured Data per Station at Sohag

Station	Distance from (L.B.)	Mean depth (m)	$d_{10}$ ( $\mu\text{m}$ )	$d_{50}$ ( $\mu\text{m}$ )	$d_{90}$ ( $\mu\text{m}$ )	Standard deviation of bed material $\sigma_g$	Mean $K_s$ (m)	Velocity		Suspended load (kg/m/s)		Bed load	
								Mean	Standard deviation	Mean	Standard deviation	Mean	Standard deviation
1	55	4.54	352	586	1155	2.0	0.29	0.82	0.0707	0.0396	0.006	0.0117	0.007
2	124	4.58	177	453	594	1.4	0.38	0.77	0.0264	0.1118	0.0633	0.0313	0.013
3	183	4.13	236	472	987	1.8	0.26	0.88	0.0512	0.1236	0.0296	0.0291	0.0037
4	274	4.19	160	258	412	1.1	0.28	0.78	0.0466	0.2199	0.0291	0.0259	0.0179
5	355	4.12	176	251	330	1.7	0.03	0.75	0.0465	0.0979	0.0168	0.01	0.0025
6	425	4.27	204	314	591	1.5	0.06	0.61	0.0326	0.0175	0.001	0.002	0.0011

**Table 5.** Measured Data per Station at Bani-Sweif

Station	Distance from (L.B.)	Mean depth (m)	$d_{10}$ ( $\mu\text{m}$ )	$d_{50}$ ( $\mu\text{m}$ )	$d_{90}$ ( $\mu\text{m}$ )	Standard deviation of bed material $\sigma_g$	Mean $K_s$ (m)	Velocity		Suspended load (kg/m/s)		Bed load	
								Mean	Standard deviation	Mean	Standard deviation	Mean	Standard deviation
1	344	2.82	306	603	1661	1.77	0.29	0.81	0.0551	0.0163	0.0029	0.0191	0.0057
2	282	2.76	415	490	1,216	1.64	0.22	0.74	0.0157	0.0272	0.0034	0.0152	0.0105
3	221	2.76	359	409	700	1.43	0.03	0.72	0.0238	0.0422	0.0029	0.0178	0.0098
4	179	3.40	305	343	543	1.39	0.09	0.66	0.0169	0.0416	0.0050	0.0126	0.0058
5	120	4.28	295	350	697	1.56	0.23	0.71	0.0258	0.0482	0.0068	0.0057	0.0021
6	60	5.04	251	296	619	1.63	0.40	0.73	0.0075	0.0623	0.0094	0.0040	0.0022

**Fig. 4.** Bed-load transport as function of current velocity; data from Nile River in Egypt and Rhine-Waal River in The Netherlands

## Results of Bed-Load Transport Data

The bed-load transport rates including variation ranges measured in the Nile River are shown in Fig. 4. As can be observed, the bed load transport rates of sediment in the range of ( $d_{50}$ ) 0.2–0.6 mm increase from about 0.0005 to about 0.05 (increase of a factor of 100) over the velocity range from 0.35 to 0.85 m/s. For comparison, similar data from the Rhine-Waal River in The Netherlands (Van Rijn 1991, 1992; Gaweesh and Van Rijn 1994) are also shown in Fig. 4. The Rhine-Waal data have been measured in depths of 4 to 5 m, with current velocities in the range of 0.45–0.9 m/s and  $d_{50}$  values of about 0.53 mm, using the same bed-load transport sampler. Individual data points of the Nile and Rhine-Waal data sets have been clustered as much as possible into data groups of current velocity and transport to reduce the scatter. Generally, the scatter of the individual transport rates is relatively large, masking a clear view of the general trend of the data. The values within the groups (based on at least 10 values within each group) have been averaged to obtain representative group-averaged values. The variation range of the velocity within a group is about 10% of the mean value; the variation range of the corresponding suspended transport rates is as large as 50%. The

variation ranges are also shown in Fig. 4 to get some idea of the scatter involved. The bed-load transport rates from both rivers show very good agreement, which gives some confidence in the quality and consistency of both data sets. The bed-load transport rates show rather good correlation with depth-mean velocity. This latter parameter was used as the independent variable because it represents a simple and accurate local variable. An alternative variable is the local shear stress, but this variable involves the estimation of local friction or local slope and associated errors (regression of measured velocity profiles or reach-average slope, etc.).

The following three formulas for the prediction of bed-load transport have been tested using the Nile data: Meyer-Peter–Muller (MPM) (1948); Bagnold (1966); and Van Rijn (1984a). These models were selected because they are well known and they represent the two main types of models: based on bed-shear stress (MPM and Van Rijn) and energy (Bagnold and Engelund–Hansen). The methods of MPM and Van Rijn are related to grain shear stress derived from flow velocity and grain roughness; the method of Bagnold is based on the stream power concept (product of bed-shear stress and flow velocity).

**Table 6.** Measured and Predicted Bed-Load Transport Rates at the Four Sites

Site	Bed-load transport rates integrated over the cross section (kg/s)			
	Measured	Predicted		
		Bagnold	MPM	Van Rijn
Aswan	1.73	8.2 (4.7)	2.9 (1.7)	1.6 (0.93)
Quena	3.21	12.8 (4.0)	5.8 (1.8)	2.7 (0.86)
Sohag	7.21	31.2 (4.3)	19.1 (2.7)	14.0 (1.9)
Bani-Sweif	3.92	22.3 (5.7)	14.4 (3.7)	11.5 (2.9)

Note: Ratio of computed and measured transport rate is given in parentheses.

Table 6 shows the comparison between the measured and predicted bed load transport rates at the four sites; the ratio of computed and measured transport rates is given between brackets. It can be concluded that the prediction formula of Van Rijn gives significantly better results than the method of Bagnold and slightly better results than the method of MPM. The method of Bagnold generally overpredicts the bed load transport rates because the overall bed-shear stress is used instead of the grain-shear stress. The method of Van Rijn underpredicts the measured rates for the two sites of Aswan and Quena with factors of 0.93 and 0.86, respectively; whereas it overpredicts the measured rates for the two sites of Sohag and Bani-Sweif with factors of 1.90 and 2.90, respectively. The other formulas used overpredict the measured rates within a factor ranging from about 2 to 5.

## Effect of Graded Sediment on Bed Load Transport

### Approach

Analysis of bed material samples shows that the bed material of the Nile River is slightly nonuniform at present; the ratio  $d_{90}/d_{50}$  has values up to 3. Selective grain transport processes may take place, involving the selective movement of sediment particles in a mixture near incipient motion at low bed-shear stresses and during generalized transport at higher shear stresses. Several effects are important: (1) the degree of exposure of sediment particles of unequal size within a mixture (hiding of smaller particles resting or moving between the larger particles); and (2) the nonlinear relationship between transport rate and particle diameter. Given these effects, the predictions of the bed-load transport rates for the Nile River may not be so accurate if they are based on a formula developed for uniform sediment.

Since the bed-load formula of Van Rijn (1984a) gave the closest values to the field measurements, it was selected to be modified by introducing a correction factor related to the size distribution (standard deviation,  $\sigma_g$ ) of the bed material. This correction factor modifies the effective bed-shear stress. The  $\sigma_g$  parameter is defined as

$$\sigma_g = \frac{d_{84}/d_{50} + d_{50}/d_{16}}{2} \quad (1)$$

with  $d_{16}$  which represents the size at which 16% by weight is finer;  $d_{50}$  which represents the size at which 50% by weight is finer, and  $d_{84}$  which represents the size at which 84% by weight is finer.

Using this approach, the weakly nonuniform bed material of the Nile River is schematized as a single fraction represented by  $d_{50}$  and  $\sigma_g$ . For strongly nonuniform bed material, it is more appropriate to use a multifraction method by schematizing the bed material into a number of size fractions and to compute the sand transport rate of each size fraction by using an existing single fraction method (replacing the median diameter of the bed material by the mean diameter of each fraction) with a correction factor acting on the critical bed-shear stress to account for the nonuniformity effects (Egiazaroff 1965; Almedeij and Diplas 2003; Roberts et al. 2003).

### Modification of Bed-Load Transport Formula

The original bed-load formula of Van Rijn (1984a,b) reads as

$$q_b = 0.053 \Delta^{0.5} g^{0.5} d_{50}^{1.5} D_*^{-0.3} T^{2.1}; \quad T < 3 \quad (2)$$

$$q_b = 0.100 \Delta^{0.5} g^{0.5} d_{50}^{1.5} D_*^{-0.3} T^{1.5}; \quad T > 3 \quad (3)$$

where  $q_b$  = volumetric bed-load transport ( $m^2/s$ );  $g$  = acceleration of gravity ( $m/s^2$ );  $d_{50}$  = sediment size at which 50% of material is finer (m);  $\Delta$  = relative density =  $s - 1 = (\rho_s - \rho)/\rho$  (-);  $D_*$  = dimensionless particle parameter (-) =  $d_{50} [(s - 1)g/\nu^2]^{1/3}$ ;  $\nu$  = kinematic viscosity coefficient ( $m^2/s$ );  $s$  = specific density =  $\rho_s/\rho$  (-);  $\rho_s$  = sediment density ( $kg/m^3$ ); and  $\rho$  = fluid density ( $kg/m^3$ )

$$T = (\tau'_b - \tau_{b,cr})/\tau_{b,cr} \quad (4)$$

$\tau'_b$  = effective bed-shear stress =  $\rho g(u/C')^2$ ;  $u$  = depth-mean flow velocity (m/s);  $C'$  = grain-related Chezy coefficient =  $18 \log(4h/d_{90})$ ;  $h$  = mean flow depth (m); and  $\tau_{b,cr}$  = critical bed-shear stress at which sediment start moving (according to Shields).

The correction of the bed-shear parameter,  $T_{modified}$  will be as follows:

$$T_{modified} = (\lambda \tau'_b - \tau_{b,cr})/\tau_{b,cr} \quad (5)$$

in which  $\lambda$  = correction factor. Basically, this factor introduces a correction of the grain roughness of a sediment mixture. The grain roughness will decrease for a wider distribution because the larger particles will be less exposed in a relatively wide mixture (smaller particles will fill the interstices between the larger particles). Therefore the  $\lambda$  factor is assumed to be related to the characteristics of the mixture.

From Eqs. (2), (3), and (4), it can be observed that

$$\lambda = \tau_{b,cr} [1 + \{q_b / (0.053 \Delta^{0.5} g^{0.5} d_{50}^{1.5} D_*^{-0.3})\}^{1/2.1}] / \tau'_b; \quad T < 3 \quad (6)$$

and

$$\lambda = \tau_{b,cr} [1 + \{q_b / (0.100 \Delta^{0.5} g^{0.5} d_{50}^{1.5} D_*^{-0.3})\}^{1/1.5}] / \tau'_b; \quad T > 3 \quad (7)$$

Hence for given  $q_b$ ,  $\Delta$ ,  $g$ ,  $d_{50}$ , and  $D_*$ , the correction factor  $\lambda$  can be determined (Amin 1999).

### Experimental Laboratory Data Set

A series of laboratory experiments was carried out in a straight flume at HRI, Delta Barrage, Egypt, under steady uniform (equilibrium) conditions. Different sizes of bed material and different flow characteristics were used in order to determine the corresponding bed-load transport rates for a variety of boundary conditions. In all, 19 flume tests were carried out. During the tests

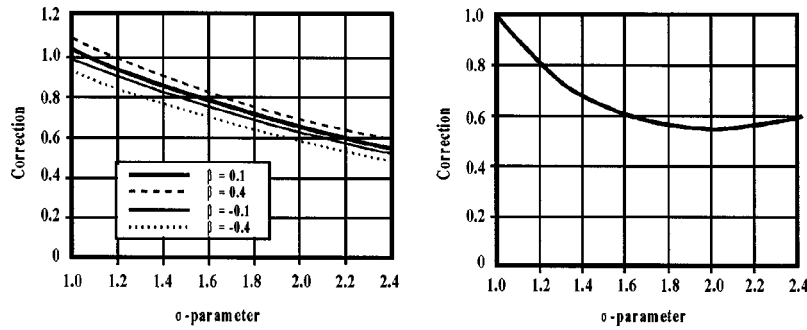


Fig. 5. Correction factor  $\lambda$ ; left: method A; and right: method B

different bed material sizes of mean particle diameter ( $d_{50}$ , ranging between 245 and 1,100  $\mu\text{m}$ ), with different grain size distribution ( $1.1 < \sigma_g < 2.5$ ), were used. The flow depths were in the range of 0.3–0.5 m and the flow velocities were in the range of 0.43–0.64 m/s. The basic data are presented by Gaweesh and Van Rijn (1994).

**Determination of Correction Factor  $\lambda$**

Based on the available laboratory data set of bed-load transport rates, the best expression for  $\lambda$  can be determined with multiple regression techniques. Two different approaches (A and B) have been followed:  $\lambda_A = f(d_{10}, d_{50}, d_{90}, \text{ and } \sigma_g)$  and  $\lambda_B = f(\sigma_g)$  resulting in

$$\lambda_A = 1 \quad (\text{no correction}) \quad \text{for } T < 2.5 \quad (8)$$

$$\lambda_A = \exp(0.45\alpha + 0.2\beta) \quad \text{for } T > 2.5 \quad (9)$$

with  $\alpha = 1 - \sigma_g$  and  $\beta = d_{50}/d_{90} - d_{10}/d_{50}$

$$\lambda_B = 1 \quad (\text{no correction}) \quad \text{for } T < 2.5 \quad (10)$$

$$\lambda_B = \exp(1.8 - 2.4\sigma_g + 0.6\sigma_g^2) \quad \text{for } T > 2.5 \quad (11)$$

As expected, the correction factor decreases with increasing standard deviation of the mixture expressing that the grain roughness

in a mixture cannot be represented with sufficient accuracy by the largest particles ( $d_{90}$ ) of the mixture. Method A is somewhat more sophisticated as the asymmetry of the sediment size distribution is taken into account, whereas method B is based on the assumption of a symmetric size distribution. Fig. 5 shows a plot of the correction factor  $\lambda$  as a function of the  $\sigma_g$  parameter for methods A and B. The  $\beta$  factor (method A) was in the range between  $-0.25$  and  $+0.25$ . The correction factor of method B increases slightly for  $\sigma_g > 2$ , which is not realistic and therefore the minimum value of  $\lambda_B (= 0.55)$  will be used for  $\sigma_g \geq 2$ .

Introducing the correction method for the Van Rijn formula, the following results can be obtained:

$$q_b = 0.053 \Delta^{0.5} g^{0.5} d_{50}^{1.5} D_*^{-0.3} T^{2.1} \quad \text{for } T < 2.5 \quad (\text{no correction}) \quad (12)$$

$$q_b = 0.100 \Delta^{0.5} g^{0.5} d_{50}^{1.5} D_*^{-0.3} (T_{\text{modified}})^{1.5} \quad \text{for } T > 2.5 \quad (13)$$

In which

$$T_{\text{modified}} = (\lambda_a \tau'_b - \tau_{b,cr}) / \tau_{b,cr} \quad \text{in the case of method A} \quad (14)$$

$$T_{\text{modified}} = (\lambda_b \tau'_b - \tau_{b,cr}) / \tau_{b,cr} \quad \text{in the case of method B} \quad (15)$$

Figs. 6 and 7 show computed and measured bed load transport

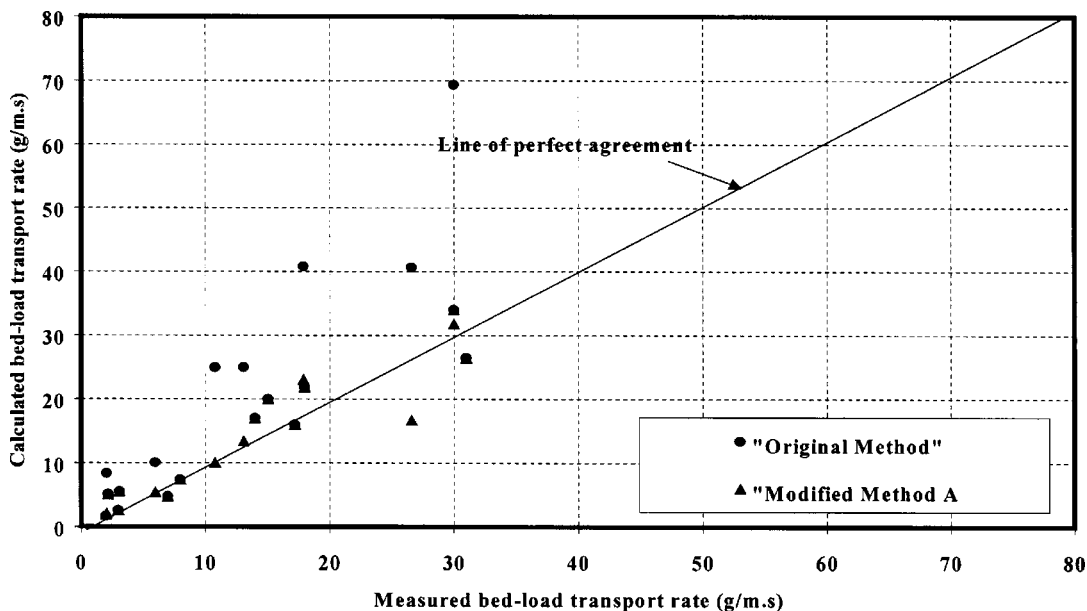


Fig. 6. Measured and computed bed-load transport rates for flume data; original method (open circles) and modified method A (triangles)

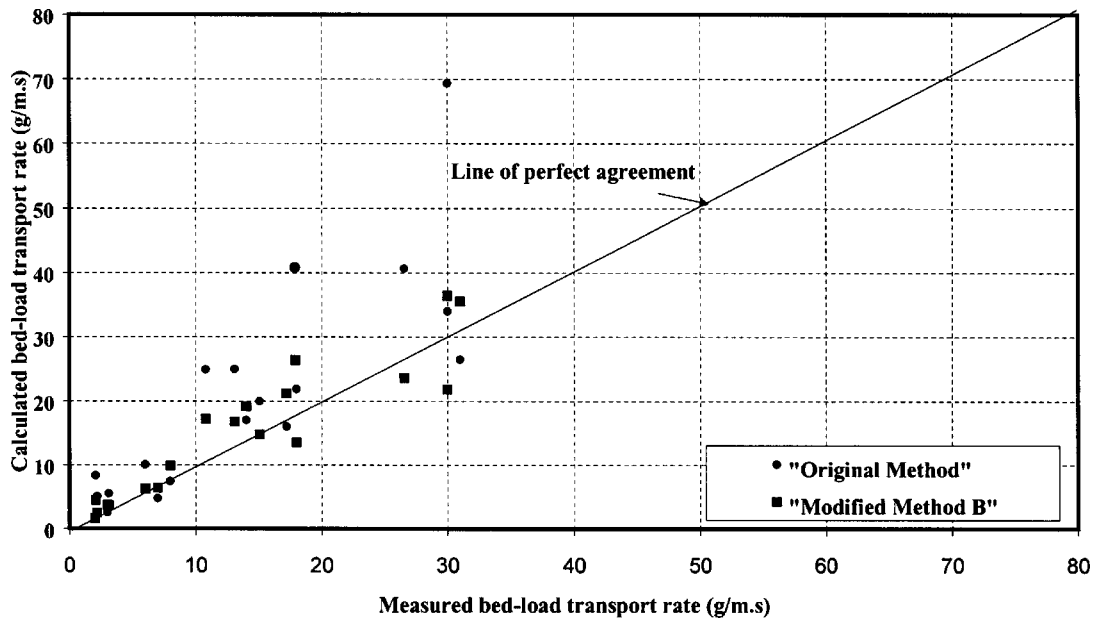


Fig. 7. Measured and computed bed-load transport rates for flume data; original method (open circles) and modified method B (squares)

rates for both approaches. Figs. 6 and 7 show that the results of the modified formula using the two approaches are quite satisfactory, as it predicts the bed-load transport rates by a factor ranging between 1 and 1.1 for approach A and 1 and 1.3 for approach B. Thus it can be concluded that the asymmetry of the sediment size distribution (method A) is important and should be taken into account.

#### Verification of Modified Bed-Load Transport Formula Using Nile Data

Since flume data have been used for calibration of the formula involved, it is necessary to make a verification with a new (inde-

pendent) data set. This verification is done by comparing the results of the modified Van Rijn formula with the measured bed load transport rates of four sites in the Nile River.

Figs. 8 and 9 show a comparison between measured bed-load transport and computed bed-load transport according to the original and the modified (A and B) Van Rijn formula. From the two figures it can be seen that:

- The modified Van Rijn formula yields values that are in better agreement with the measured values than the original formula; and
- The predictions of modified Van Rijn formula are rather good for  $T < 3$ ; but not as good for  $T > 3$ .

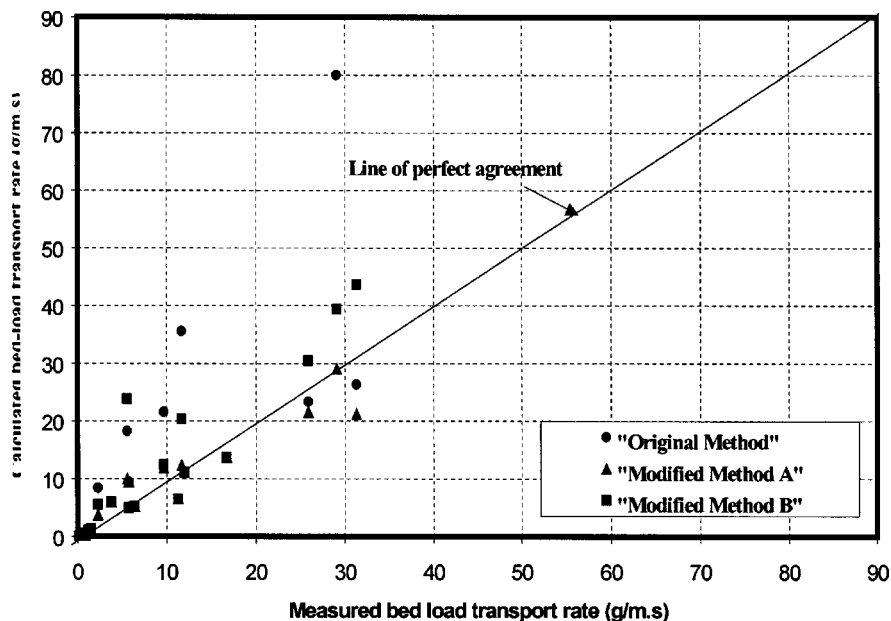


Fig. 8. Comparison of measured and computed bed-load transport for Nile data; original method (circles) and modified methods A and B (triangles and squares)

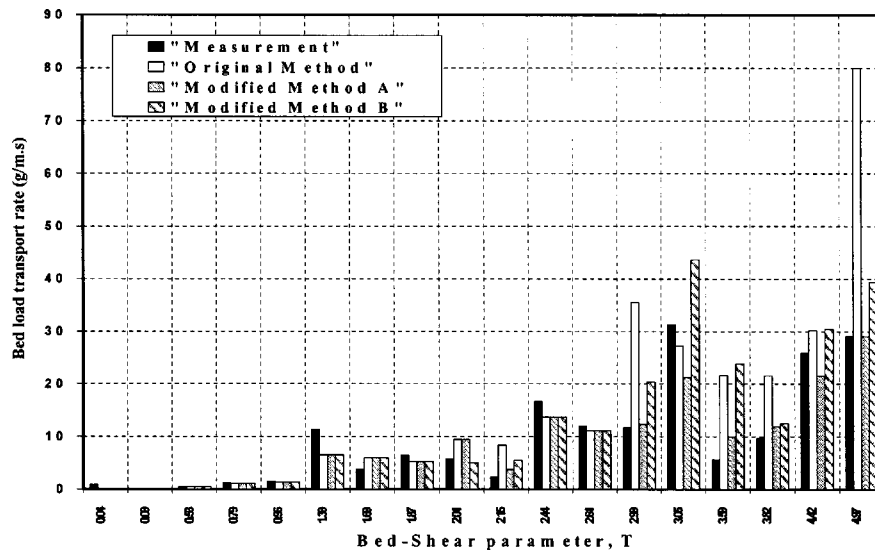


Fig. 9. Measured and computed bed-load transport versus bed shear parameter  $T$  for Nile data; original method and modified methods A and B

The following equation was used to calculate the percentage of the relative errors of the predicted values with respect to the measured values:

$$\text{relative error\%} = \text{absolute of} \left( \frac{q_{b,\text{measured}} - q_{b,\text{predicted}}}{q_{b,\text{measured}}} \times 100 \right) \quad (16)$$

in which  $q_{b,\text{measured}}$  = measured bed load transport rates; and  $q_{b,\text{predicted}}$  = predicted bed-load transport rates. The results are presented in Table 7.

Table 7 shows that the modified formula based on method A or B has an average relative error equal to 29 or 39% which is much less than the relative error of 65% of the original formula. Thus the modified Van Rijn formula shows quite good performance in predicting the bed-load transport rates for conditions with slightly nonuniform bed material as present in the Nile River in Egypt. Method A is proposed as the best correction factor for conditions with weakly nonuniform bed material. This analysis shows that the accuracy of bed-load transport formulas for uniform sediment can be improved by taking the nonuniformity effects into account.

## Analysis of Suspended Sand Transport Data

### Measured Transport Rates

The depth-integrated suspended transport rates measured in the Nile River are shown in Fig. 10 for two sediment size classes ( $d_{50}$ ) of 0.2–0.4 mm and 0.4–0.6 mm. For comparison, similar data from the Mississippi River in the USA (Peterson and Howells 1973) are also presented in Fig. 10. The Mississippi data have been measured in depths of 1.0–11.0 m, with current velocities in

the range of 0.6–2.0 m/s and  $d_{50}$  values in the range of 0.2–0.6 mm. Individual data points of the Nile and Mississippi River data sets have been clustered as much as possible into data groups of current velocity to reduce the scatter. The values within the groups have been averaged to obtain representative group-averaged values. The transport rates of the Nile data set are in the lower velocity regime (0.3–0.8 m/s), while the values of the Mississippi data set are in the upper velocity regime (0.7–2.0 m/s). Overlapping transport data can be observed around velocities of 0.7 to 0.8 m/s for  $d_{50}$  values in the range of 0.2–0.4 mm (upper plot of Fig. 10). The data points of both data sets are complementary and show a very consistent trend of suspended transport against current velocity; transport is roughly proportional to  $(V_{av})^4$  for velocities smaller than 1 m/s and  $(V_{av})^3$  for velocities larger than 1 m/s. This change in the slope of the suspended transport versus velocity plot is probably caused by the effect of the suspended sediment on the turbulence mixing capacity in the high-velocity range (turbulence damping effect; Van Rijn 1993b).

### Analysis of Concentration Profiles of Nile River

Adopting the sediment diffusivity theory based on a parabolic distribution over the depth, the relative sediment concentration profile can be expressed by the well-known Rouse concentration profile

$$C/C_a = \left\{ \left[ \frac{(h-y)/y}{a/(h-a)} \right] \right\}^Z \quad (17)$$

in which  $C$  = sand concentration at height  $y$  above the bed ( $\text{kg}/\text{m}^3$ );  $C_a$  = reference sand concentration ( $\text{kg}/\text{m}^3$ );  $Z$  = suspension number or  $Z$  parameter ( $-$ ) =  $W_s / (\beta \kappa u_*^-)$ ;  $W_s$  = fall velocity of suspended sediment (m/s);  $\beta$  = ratio of sediment and fluid momentum diffusivity coefficient ( $-$ );  $\kappa$  = Von Karman coefficient ( $-$ ); and  $u_*^-$  = bed-shear velocity (m/s).

Analysis of the measured and predicted concentration profiles was carried out for all data of the four measurement sites to determine the two basic parameters:  $Z$  and  $C_a$ . To reduce the variation within the dataset, the measured concentration profiles were clustered into two depth classes ( $h = 2.0$ – $4.5$  and  $4.5$ – $6.5$  m) and three current velocity classes (0.2–0.45, 0.45–0.7, and 0.7–0.95 m/s). Averages and standard deviations were computed

Table 7. Percentage of the Relative Errors for Different Approaches

Approach	Relative error %		
	Minimum	Average	Maximum
Van Rijn (1984a)	0.60	65	224
Van Rijn Model A	0.18	29	92
Van Rijn Model B	0.60	39	140



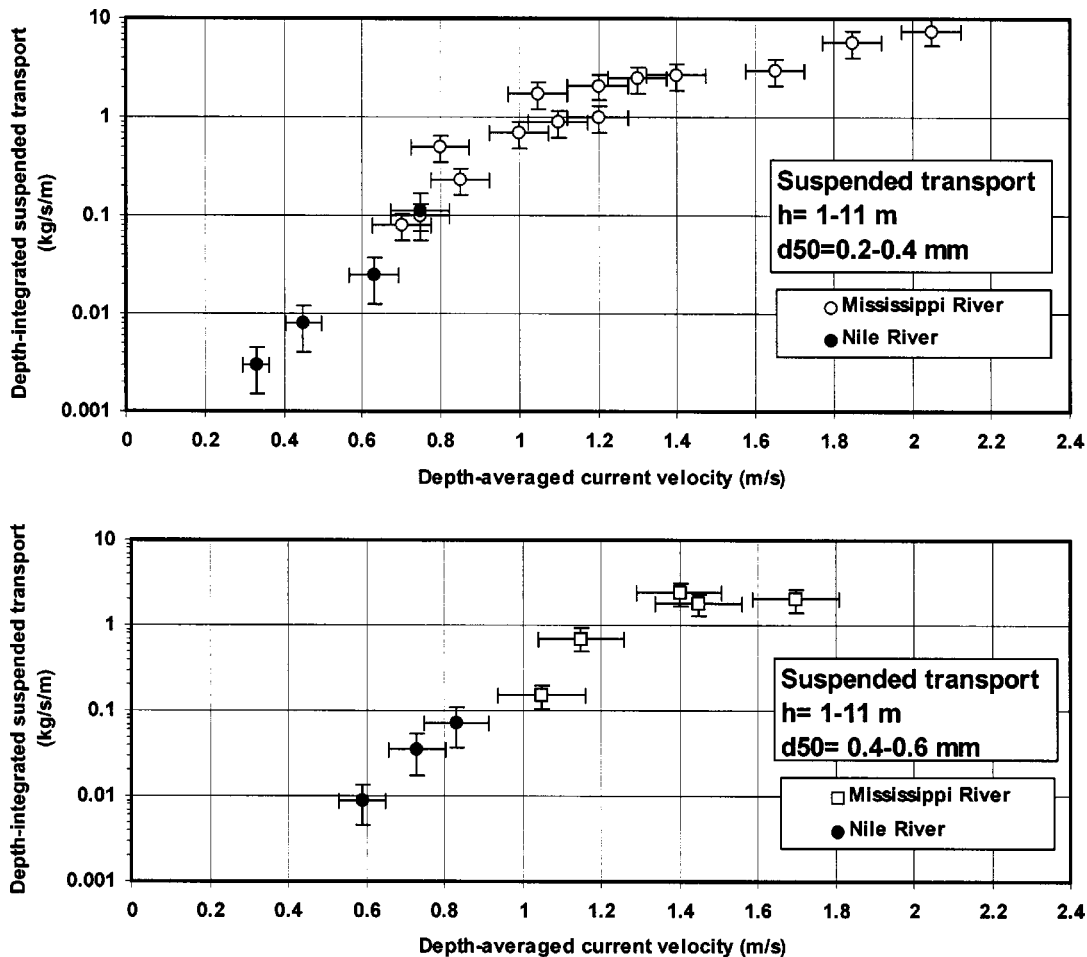


**Fig. 10.** Suspended transport as function of current velocity; data from Nile River in Egypt and Mississippi River in the USA; upper:  $d_{50}$  between 0.2 and 0.4 mm; lower:  $d_{50}$  between 0.4 and 0.6 mm

for all parameters within each class, see Table 8. Some of the average concentration profiles including standard error ranges are shown in Fig. 11, where the standard error is equal to the standard deviation divided by the square root of the number of concentrations within the class. The error of individual data points is about a factor of 2.

The  $Z_{meas}$  parameter derived from the measured concentration profiles by using a fitting procedure is given in Table 8. The predicted  $Z_{predic}$  parameter is defined as  $Z_{predic} = W_s / (\beta \kappa u_*')$  with  $W_s$  = fall velocity based on bulk samples of suspended sediment,  $\beta = 1$ ,  $\kappa = 0.4$ , and  $u_*'$  = bed-shear velocity derived from measured velocity profiles (by fitting). The  $Z_{predic}$  values are also given in Table 8. The  $Z_{meas}$  parameters range between 0.3 and 0.8, whereas the  $Z_{predic}$  parameters range from 0.7 to 2.7. This significant discrepancy cannot be explained from the fitting procedure itself but only from the parameters of the  $Z_{predic}$  parameter: the measured fall velocity  $W_s$  may be too large, the bed-shear velocity  $u_*'$  may be too small, and/or the  $\beta$  value may be much larger than 1. This latter option is in line with the results of Coleman (1970) yielding values between 1 and 2 (see Van Rijn 1993b). The reason for  $\beta > 1$  is explained by the presence of eddy-induced centrifugal forces acting on the sand particles (of larger density) and causing the particles to be thrown to the outside of the eddies with a consequent increase of the effective mixing length and hence diffusivity. A more detailed study including statistics is required to identify the proper causes for the observed discrepan-

cies of the  $Z$  parameter. The present results should be seen as a first exploratory study of the parameters involved.

Measured  $C_a$  values were compared to computed values based on Van Rijn (1984b) as follows:

$$C_a = 0.015(d_{50}/a)(T^{1.5}/D_*^{0.3}) \quad (18)$$

where  $a$  = reference level above the mean bed (m);  $D_*$  = dimensionless particle parameter (-); and  $T$  = dimensionless bed-shear parameter (-).

The reference level ( $a$ ) was assumed to be equal to the bed-roughness height ( $k_s$ , value =  $30z_0$  with  $z_0$  = zero velocity level), derived from the measured velocity profiles (zero-velocity level, see Tables 2–5). The measured  $C_a$  values were determined from the measured concentration profiles by interpolation taking the  $a$  value equal to the bed roughness height ( $k_s$ ). The measured and predicted  $C_a$  values are given in Table 8. The measured  $C_a$  values are in the range between 0.01 and 0.15 kg/m<sup>3</sup>. Some results are conflicting; for example, the measured  $C_a$  at the Bani Sweif site is 0.1 kg/m<sup>3</sup> and 0.02 kg/m<sup>3</sup> at Sohag for the same depth and velocity class (depth = 2.5–4.5 m; velocity = 0.45–0.70 m/s). Thus a variation of a factor 5 may easily occur for similar conditions, which stresses the variability of local near-bed conditions. The predicted values, which represent a spatial averaged value along the bed forms, are considerably larger than the measured local values (factor 1–10; factor 3 averaged over all data). Further

**Table 8.** Average Values of Suspension Parameters in Nile River

Site	Depth range (m)	Velocity range (m/s)	Median particle size $d_{50}$ (mm)		Bed roughness $k_s$ (m)		Bed shear velocity $U_*$ (m/s)		Measured				Predicted		
			Average	Standard	Average	Standard	Average	Standard	$C_{a,meas}$		$Z_{meas}$		$C_{a,predic}$	$Z_{predic}$	
									Average	Standard	Average	Standard			Average
Bani-Sweif	2.5–4.5	0.20–0.45	—	—	—	—	—	—	—	—	—	—	—	—	—
		0.45–0.70	350	28	0.073	0.062	0.052	0.003	0.10	0.062	0.426	0.079	0.11	0.81	
		0.70–0.95	476	96	0.160	0.126	0.05	0.005	0.09	0.043	0.427	0.143	0.37	0.85	
	4.5–6.5	0.20–0.45	—	—	—	—	—	—	—	—	—	—	—	—	—
		0.45–0.70	—	—	—	—	—	—	—	—	—	—	—	—	—
		0.70–0.95	296	0	0.478	0.037	0.06	0.001	0.05	0.01	0.409	0.053	0.14	0.66	
Aswan	2.5–4.5	0.20–0.45	—	—	—	—	—	—	—	—	—	—	—	—	—
		0.45–0.70	—	—	—	—	—	—	—	—	—	—	—	—	—
		0.70–0.95	—	—	—	—	—	—	—	—	—	—	—	—	—
	4.5–6.5	0.20–0.45	340	11	0.183	0.101	0.026	0.006	0.01	0.002	0.313	0.053	0.	2.46	
		0.45–0.70	390	84	0.056	0.047	0.028	0.01	0.01	0.003	0.373	0.087	0.16	2.37	
		0.70–0.95	—	—	—	—	—	—	—	—	—	—	—	—	—
Sohag	2.5–4.5	0.20–0.45	—	—	—	—	—	—	—	—	—	—	—	—	—
		0.45–0.70	314	0	0.059	0.043	0.033	0.006	0.02	0.003	0.395	0.037	0.27	2.13	
		0.70–0.95	374	120	0.119	0.095	0.054	0.016	0.15	0.123	0.502	0.124	0.31	1.37	
	4.5–6.5	0.20–0.45	—	—	—	—	—	—	—	—	—	—	—	—	—
		0.45–0.70	—	—	—	—	—	—	—	—	—	—	—	—	—
		0.70–0.95	552	57	0.340	0.166	0.06	0.004	0.03	0.023	0.416	0.154	0.15	1.13	
Quena	2.5–4.5	0.20–0.45	253	14	0.018	0.012	0.023	0.007	0.01	0.004	0.611	0.034	0.	2.72	
		0.45–0.70	300	46	0.087	0.071	0.035	0.011	0.02	0.013	0.620	0.163	0.11	1.79	
		0.70–0.95	—	—	—	—	—	—	—	—	—	—	—	—	—
	4.5–6.5	0.20–0.45	—	—	—	—	—	—	—	—	—	—	—	—	—
		0.45–0.70	282	0	0.017	0.007	0.037	0.01	0.06	0.020	0.777	0.029	0.2	1.65	
		0.70–0.95	—	—	—	—	—	—	—	—	—	—	—	—	—

studies are necessary to identify the effect of nonuniformity of the bed material on the  $Z$  and  $C_a$  parameters.

### Comparison of Measured and Predicted Suspended Transport Rates

The suspended-load transport rates were computed using the prediction methods of Bagnold (1966) and Van Rijn (1984b). These models were selected because they are well-known and they represent the two main types of models: based on bed-shear stress (Van Rijn) and energy (Bagnold). Table 9 shows the comparison between the measured and predicted suspended-load transport rates at the four sites; the ratio of computed and measured transport rates is given between brackets. It can be concluded that the prediction formula of (Van Rijn) underpredicts the measured rates for the three sites of Aswan, Quena, and Sohag with factors of 0.4–0.7, respectively; whereas it overpredicts the measured rates for the site of Bani-Sweif with a factor of 1.6. The prediction formula of (Bagnold) overpredicts the measured rates for the three sites of Aswan, Quena, and Bani-Sweif with factors of 1.1 to 1.2, respectively; whereas it underpredicts the measured rates for the site of Sohag with a factor of 0.55. These results show that the suspended transport rates of both formulas are in quite good agreement with the measured values.

### Comparison of Measured and Predicted Total Load Transport Rates

The total load transport rates were computed using the prediction method of Engelund–Hansen (1967), see Table 10. This model

was selected because it is well-known and it represents the energy type of models. Furthermore, it gets around the problem of bed-load and suspended-load definitions. The results of the methods of Bagnold and Van Rijn are also given. Table 10 shows the comparison between the measured and predicted total load transport rates at the four sites; the ratio of computed and measured transport rates is given between brackets. It can be concluded that the prediction formula of Bagnold slightly overpredicts the measured values; and the method of Van Rijn tends to underpredict the measured results. The method of Engelund–Hansen gives consistent results with Bagnold formula and slightly overpredicts the measured values. The three used methods revealed good results; all computed transport rates are within a factor of about 2 of the measured values. It can be concluded that the prediction formula of (Van Rijn) underpredicts the measured rates for the three sites of Aswan, Quena, and Sohag with factors of 0.6–0.9, respectively; whereas it overpredicts the measured rates for the site of Bani-Sweif with a factor of 1.9. The prediction formulas of (Bagnold) and (Engelund–Hansen) overpredict the measured rates for the four sites with factors of 1 to about 2.2.

### Conclusions

Measurements of sediment-load transport rates were carried out successfully at four cross sections on the Nile River, in Egypt, along the entire length from Aswan to Cairo using a mechanical sampler called the Delft Nile Sampler. Based on analysis results of the data, the following conclusions are given:

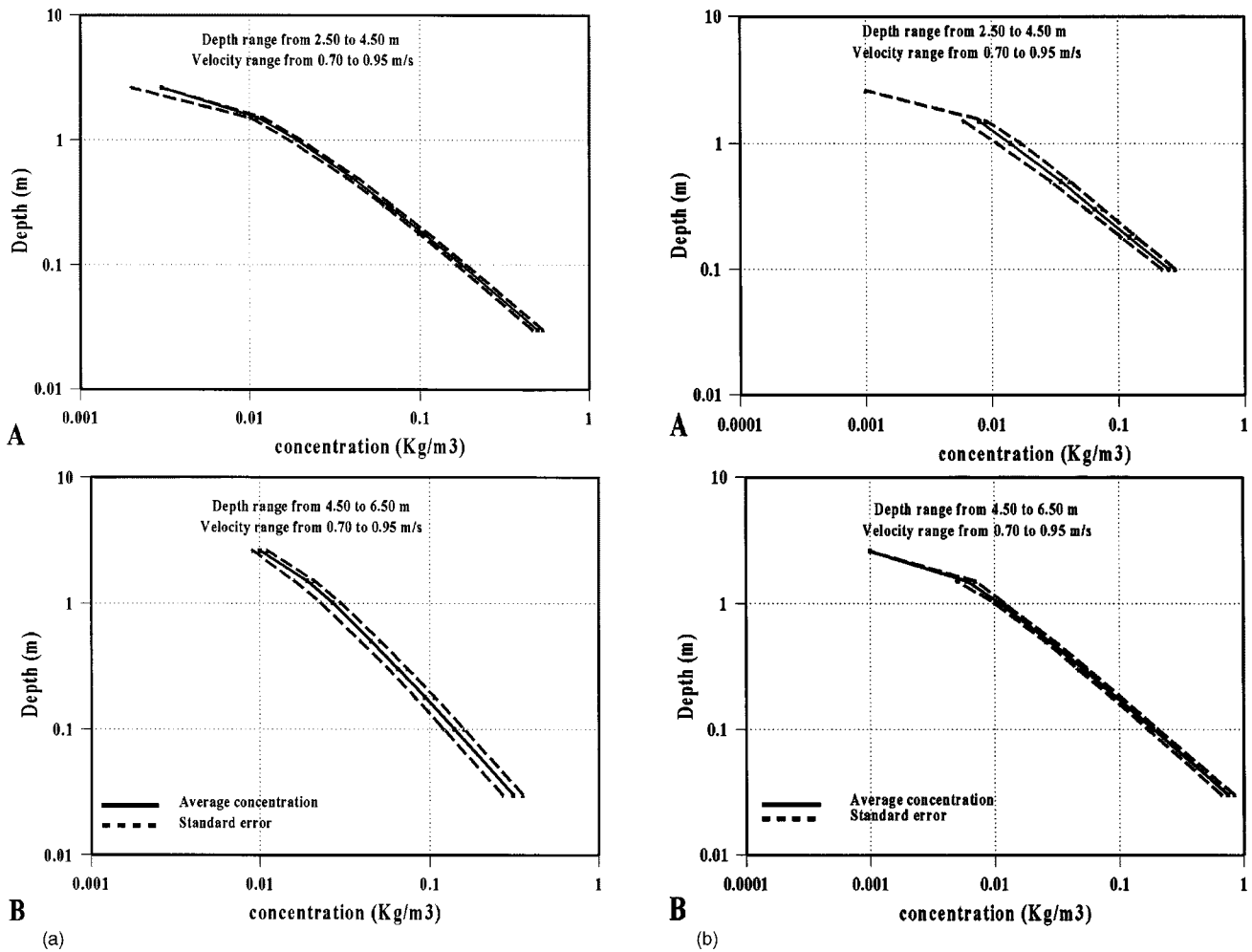


Fig. 11. Concentration profiles at (a) Bani Sweif, and (b) Sohag

1. Comparison of measured and predicted bed-load transport rates shows that, for the Nile river, the bed-load formula of Van Rijn (1984a) gives values which are in good agreement with the measured bed-load transport rates; the average relative error is about 60%.
2. Modification of the Van Rijn formula (1984a) was performed to extend it to conditions with slightly nonuniform sediment

3. Comparison of bed-load transport measured in the Nile River with computed transport rates of the modified formula show improved results; the average relative error is

**Table 9.** Measured and Predicted Suspended-Load Transport Rates at the Four Sites (Ratio of Computed and Measured Transport Rate is given between Brackets)

Site	Suspended-load transport rates integrated over the cross section (kg/s)		
	Measured	Predicted	
		Bagnold (1996)	Van Rijn (1984a,b)
Aswan	4.4	4.9 (1.1)	1.8 (0.4)
Quena	8.9	10.1 (1.1)	6.6 (0.7)
Sohag	47.9	26.3 (0.6)	34 (0.7)
Bani-Sweif	15.8	18.5 (1.2)	25 (1.6)

**Table 10.** Measured and Predicted Total Load Transport Rates at the Four Sites (Ratio of Computed and Measured Transport Rate is Given between Brackets)

Site	Total load transport rates integrated over the cross section (kg/s)			
	Measured	Predicted		
		Bagnold	Engelund-Hasen	Van Rijn
Aswan	6.1	13.2 (2.2)	7.4 (1.2)	3.4 (0.6)
Quena	12.1	23.0 (1.9)	19.7 (1.6)	9.4 (0.8)
Sohag	55.1	57.5 (1.05)	66.2 (1.2)	48.0 (0.9)
Bani-Sweif	19.7	40.8 (2.1)	43.3 (2.2)	36.9 (1.9)

about 30%.

4. Comparison of bed-load transport rates measured in the Nile River with similar data from the Rhine-Waal River in the Netherlands shows very good agreement, which gives some confidence in the quality of both data sets.
5. Comparison of depth-integrated suspended transport rates measured in the Nile River with similar data from the Mississippi River in the USA shows that both data sets are complementary, revealing a very consistent trend of suspended transport against current velocity; transport is roughly proportional to  $(V_{av})^3$  to  $^4$ .
6. Analysis of measured and predicted concentration profiles of the Nile River shows that the computed suspension number  $Z$  is much larger than the measured one. This can be explained by assuming that the diffusivity of fine sand particles is much larger than the diffusivity of fluid momentum.
7. Comparison of suspended transport rates measured in the Nile River with computed suspended transport rates shows that the formulas of Bagnold and Van Rijn yield good results; all computed transport rates are within a factor of 2 of measured values; the formula of Bagnold performs slightly better.
8. Comparison of the total load transport rates measured in the Nile River with computed total load transport rates shows that the formulas of Bagnold, Van Rijn, and Engelund-Hansen yield good results; all computed transport rates are within a factor of about 2 of measured values.

## Acknowledgments

This research program was conducted within the research plan of the Hydraulics Research Institute, National Water Research Center, Delta Barrage, Egypt. The work was carried out in cooperation with Delft Hydraulics through the framework of the Netherlands Technical Assistance Project funded by the Dutch government. Dr. M. T. K. Gaweesh, Director of the Hydraulics Research Institute, was the principal investigator through the developing stage of the Delft Nile Sampler in addition to its calibration and verification (1987–1992). Dr. M. B. A. Saad, Former Director of the Hydraulics Research Institute, Egypt, is gratefully acknowledged for his support and encouragement.

## Notation

The following symbols are used in this paper:

- $a$  = reference level above mean bed;
- $C$  = sand concentration at height  $y$  above bed;
- $C'$  = grain-related Chezy coefficient;
- $C_a$  = reference sand concentration;
- $D_*$  = dimensionless particle parameter;
- $d_{10}$  = sediment size at which 10% by weight is finer;
- $d_{16}$  = sediment size at which 16% by weight is finer;
- $d_{50}$  = sediment size at which 50% by weight is finer;
- $d_{84}$  = sediment size at which 84% by weight is finer;
- $g$  = acceleration of gravity;
- $h$  = mean flow depth;
- $k_s$  = effective bed roughness height;
- $q_b$  = volumetric bed load transport;
- $s$  = specific density;
- $T$  = dimensionless bed-shear parameter;
- $T_{\text{modified}}$  = correction of the bed-shear parameter;
- $u$  = depth-mean flow velocity;

- $u^*$  = bed-shear velocity;
- $W_s$  = fall velocity of suspended sediment;
- $Z$  = suspension number or  $Z$  parameter;
- $\beta$  = ratio of sediment and fluid momentum diffusivity coefficient;
- $\Delta$  = relative density;
- $\kappa$  = Von Karman coefficient;
- $\lambda$  = correction factor;
- $\nu$  = kinematic viscosity coefficient;
- $\rho_s$  = sediment density;
- $\rho$  = fluid density;
- $\sigma_g$  = standard deviation of bed material;
- $\tau_{cr}$  = critical bed-shear stress at which sediment start moving (according to Shields); and
- $\tau'_b$  = effective bed-shear stress.

## References

- Abdel-Fattah, S. (1997a). "Field measurements of sediment load transport in the Nile river at Quena." *Technical Rep.*, Hydraulics Research Institute, HRI, Delta Barrage, Egypt.
- Abdel-Fattah, S. (1997b). "Field measurements of sediment load transport in the Nile river at Sohag." *Technical Rep.*, Hydraulics Research Institute, HRI, Delta Barrage, Egypt.
- Abdel-Fattah, S. (1997c). "Field measurements of sediment load transport in the Nile river at El-Korimat (Beni-Sweif), Report 2." *Technical Rep.*, Hydraulics Research Institute, HRI, Delta Barrage, Egypt.
- Abdel-Fattah, S. (1997d). "Field measurements of sediment load transport in the Nile river at Aswan." *Technical Rep.*, Hydraulics Research Institute, HRI, Delta Barrage, Egypt.
- Almedeij, J. H., and Diplas, P. (2003). "Bedload transport in gravel-bed streams with unimodal sediment." *J. Hydraul. Eng.*, 129(11), 896–904.
- Amin, A. M. A. (1999). "Experimental approach to bed load transport of slightly non-uniform sediment." MSc thesis H.E. 048, International Institute for Hydraulic and Environmental Engineering, IHE, Delft, The Netherlands.
- Bagnold, R. A. (1966). "An approach to the sediment transport problem from general physics." *U.S. Geol. Survey Prof. Paper 422-I*, Washington.
- Coleman, N. L. (1970). "Flume studies of the sediment transfer coefficient." *Water Resour. Res.*, 6(3).
- Egiazaroff, I. V. (1965). "Calculation of non-uniform sediment concentrations." *J. Hydraul. Div., Am. Soc. Civ. Eng.*, 91(4), 225–247.
- Engelund, F., and Hansen, E. (1967). *A monograph on sediment transport in alluvial streams*, Teknisk Forlag, Copenhagen, Denmark.
- Gaweesh, M. T. K., and Gasser, M. M. (1991). "Geomorphic and hydraulic response of the Nile River to the operation of High Aswan Dam." *Water Science Magazine*, 9, National Water Research Center, Egypt.
- Gaweesh, M. T. K., Ramadan, K. A., and El-Balasy, A. (1994). "Field measurements of sediment load transport in the Nile river at El-Korimat (Beni-Sweif)." *Technical Rep.*, Hydraulics Research Institute, HRI, Delta Barrage, Egypt.
- Gaweesh, M. T. K., and Van Rijn, L. C. (1994). "Bed load sampling in sand-bed rivers." *J. Hydraul. Eng.*, 120(12), 1364–1384.
- Kleinhans, M. G., and Ten Brinke, W. B. M. (2001). "Accuracy of cross-channel sampled sediment transport in large sand-gravel-bed rivers." *J. Hydraul. Eng.*, 127(4), 258–269.
- Meyer-Peter, E., and Muller, R. (1948). "Formulae for bed load transport." *Int. Association of Hydraulic Research 2d Meeting*, Stockholm.
- Peterson, A. W., and Howells, R. F. (1973). "Compendium of solids transport data for mobile boundary data." *Rep. No. HY-1973-ST3*, University of Alberta, Dept. of Civil Eng.
- Roberts, J. D., Jepsen, R. A., and James, S. C. (2003). "Measurements of sediment erosion and transport with the adjustable shear stress erosion and transport flume." *J. Hydraul. Eng.*, 129(11), 862–871.

- Van Rijn, L. C. (1984a). "Sediment transport, Part I: Bed load transport." *J. Hydraul. Eng.*, 110(10), 1431–1456.
- Van Rijn, L. C. (1984b). "Sediment transport, Part II: Suspended load transport." *J. Hydraul. Eng.*, 110(11), 1613–1641.
- Van Rijn, L. C. (1990). *Principles of fluid flow and surface waves in rivers, estuaries, seas and oceans*, Aqua Publications, Amsterdam, The Netherlands.
- Van Rijn, L. C. (1991). "Bed load transport measurements in the River Waal." *Rep. No. Q1300*, Delft Hydraulics, Delft, The Netherlands.
- Van Rijn, L. C. (1992). "Bed load transport measurements in the River Waal near Duten, near Woudrichem." *Rep. No. Q1300 part II and III*, Delft Hydraulics, Delft, The Netherlands.
- Van Rijn, L. C. (1993a). "Manual sediment transport measurements." *Rep.*, Delft Hydraulics, Delft, The Netherlands.
- Van Rijn, L. C. (1993b). *Principles of sediment transport in rivers, estuaries, coastal seas and oceans*, Aqua Publications, Amsterdam, The Netherlands.
- Van Rijn, L. C., and Gaweesh, M. T. K. (1992). "New total sediment load sampler." *J. Hydraul. Eng.*, 118(12), 1686–1691.